International Journal of Environmental Sciences
ISSN: 2229-7359
Vol. 11 No. 21s, 2025
https://theaspd.com/index.php

Development And Characterization of Garlic (Allium Sativum) Extract-Loaded Biodegradable Nanoparticles For Targeted Antibacterial and Antiviral Therapy in Acute and Chronic Respiratory Infections

Mhaveer Singh[1], N Ramasamy[2], Jaswinder Kaur[3], Aarush Keserwal[4], Vaishali Ramesh Patil[5], V Pradeepa[6], M Sujatha[7], Pyrkhatlang Myrboh[8], M Kiruthika[*9]

[1]Associate Professor, School of Pharmaceutical Sciences, Faculty of Pharmacy, IFTM University, Moradabad, Uttar Pradesh, India

[2]Professor, Department of Pharmacognosy, S. A. Raja Pharmacy College, Vadakkankulam, Tirunelveli, Tamilnadu, India

[3]Medical lab Sciences, Chandigarh School of Business, Chandigarh Group of Colleges Jhanjeri, Mohali, Punjab, India

[4]Research Scholar, Teerthanker Mahaveer college of Pharmacy, Teerthanker Mahaveer University, Moradabad ,Uttar Pradesh, India

[5]Assistant Professor, Department of Pharmaceutical Quality Assurance, Hon. Tukaramsheth S. Baviskar Institute of Pharmaceutical Education and Research Dahiwad, Shirpur, India

[6]Assistant Professor, Department of Biotechnology, Sri Kaliswari College, Tamil Nadu, India

[7]Head & Assistant Professor, Department of Biotechnology, Sri Kaliswari College, Tamil Nadu, India

[8]Assistant Professor, Department of Pharmacognosy, University of Science and Technology Meghalaya, India

[9]Assistant Professor, Department of Chemistry, Arignar Anna Government Arts College, Musiri, Tamilnadu, India

*Corresponding Author : M Kiruthika, Assistant Professor, Department of Chemistry, Arignar Anna Government Arts College, Musiri, Tamilnadu, India, kiruthikagac15@gmail.com

Abstract

Background:*Respiratory infections, both acute and chronic, remain major global health burdens exacerbated by antimicrobial resistance and limited antiviral options. Garlic (Allium sativum) possesses broad-spectrum antimicrobial and antiviral activities but suffers from poor stability and bioavailability. Nanoparticle-based delivery systems can potentially enhance its therapeutic efficacy.*

Objective:*To develop and characterize biodegradable nanoparticles loaded with garlic extract for targeted antibacterial and antiviral therapy in respiratory infections, and to evaluate their cytotoxicity.*

Methods: *Garlic extract-loaded biodegradable nanoparticles were prepared using the solvent evaporation method and characterized for particle size, polydispersity index (PDI), zeta potential, morphology (SEM/TEM), encapsulation efficiency, drug loading, FTIR spectra, DSC/XRD profiles, and in vitro release in simulated lung fluid. Antibacterial activity was assessed using agar well diffusion, MIC/MBC determination, and time-kill kinetics. Antiviral potential was evaluated via plaque reduction assay, viral inhibition percentage calculation, and CPE inhibition assay. Cytotoxicity was tested on A549 cells using the MTT assay. Data were analyzed by one-way ANOVA with Tukey's post-hoc test ($p < 0.05$).*

Results:*The optimized nanoparticles exhibited an average size of 165 ± 8 nm, PDI of 0.21 ± 0.02, and zeta potential of −22.6 ± 1.4 mV, with encapsulation efficiency of 82.4 ± 2.3% and drug loading of 16.7 ± 1.1%. FTIR, DSC, and XRD confirmed successful encapsulation and reduced crystallinity. In vitro release showed sustained garlic bioactive release over 72 h. Nanoparticles displayed lower MIC/MBC values and larger inhibition zones compared to free garlic extract. Antiviral assays revealed >70% plaque reduction and significant CPE inhibition. Cytotoxicity testing indicated >80% cell viability at therapeutic concentrations, with a favorable selectivity index.*

Conclusion:

Garlic extract-loaded biodegradable nanoparticles enhanced antibacterial and antiviral efficacy with minimal cytotoxicity, suggesting their potential as a dual-action therapeutic platform for managing respiratory infections. Further in vivo and pharmacokinetic studies are recommended.

Keywords:*Allium sativum, biodegradable nanoparticles, antibacterial activity, antiviral therapy, respiratory infections, cytotoxicity, drug delivery, phytomedicine.*

1. INTRODUCTION

1.1 Background

Acute and chronic respiratory infections remain among the leading causes of morbidity and mortality worldwide, affecting millions of individuals annually and exerting a significant socio-economic burden on healthcare systems (World Health Organization [WHO], 2023). These infections are caused by a wide range of bacterial and viral pathogens, including Streptococcus pneumoniae, Haemophilus influenzae, Mycobacterium tuberculosis, influenza viruses, respiratory syncytial virus (RSV), and coronaviruses (Troeger et al., 2018). Despite advances in antimicrobial therapy, treatment outcomes are often compromised by increasing antimicrobial resistance (AMR), limited drug bioavailability at the infection site, and adverse drug reactions (Ventola, 2015; O'Neill, 2016). The emergence of multidrug-resistant (MDR) bacterial strains and antiviral resistance in influenza and other viral pathogens underscores the urgent need for alternative therapeutic strategies (Graham et al., 2021).

Allium sativum (garlic) has been recognized for centuries as a medicinal plant with broad-spectrum antimicrobial properties. Its therapeutic activity is primarily attributed to organosulfur compounds, notably allicin, ajoene, diallyl disulfide, and S-allyl cysteine, which possess potent antibacterial, antiviral, antifungal, and immunomodulatory effects (Ankri & Mirelman, 1999; Bayan et al., 2014). Allicin, a thiosulfinate, is produced enzymatically from alliin upon garlic tissue disruption and has been shown to inhibit essential microbial enzymes and interfere with viral replication (Miron et al., 2000). These bioactive molecules are, however, chemically unstable and susceptible to degradation during processing, storage, and gastrointestinal transit, which limits their therapeutic potential in conventional formulations (Iciek et al., 2009).

1.2 Rationale

Nanoparticle-based drug delivery systems have emerged as a promising strategy to overcome the limitations of conventional antimicrobials by enhancing drug solubility, stability, bioavailability, and targeted delivery (Gupta et al., 2022). In respiratory diseases, nanoparticles can provide controlled and sustained release, improve penetration into pulmonary tissues, and facilitate targeted delivery to infected cells, thereby maximizing therapeutic efficacy while minimizing systemic side effects (Ding et al., 2019). Biodegradable polymers such as poly(lactic-co-glycolic acid) (PLGA) and chitosan are widely recognized as safe and biocompatible carriers approved for pharmaceutical use (Danhier et al., 2012). PLGA provides sustained release and protects bioactive compounds from premature degradation, while chitosan offers mucoadhesive properties that enhance retention in respiratory mucosa and facilitate penetration across epithelial barriers (Kean & Thanou, 2010).

To date, no widely reported formulation has successfully encapsulated A. sativum extract into biodegradable nanoparticles for the dual purpose of antibacterial and antiviral therapy in respiratory infections. This approach could combine the broad-spectrum efficacy of garlic phytochemicals with the pharmacokinetic advantages of nanoparticle delivery, offering a novel and potentially more effective therapeutic strategy.

1.3 Objective

Primary Objective:

- To develop and characterize Allium sativum extract-loaded biodegradable nanoparticles.

Secondary Objective:

- To evaluate their antibacterial and antiviral activities against selected respiratory pathogens.

2. MATERIALS AND METHODS

2.1 Materials

Fresh garlic (Allium sativum L.) bulbs were procured from a certified local herbal market in India and authenticated by a qualified botanist, where a voucher specimen was deposited for future reference. Analytical-grade solvents and reagents were used, including ethanol (Merck, India), dichloromethane (DCM; SRL, India), polyvinyl alcohol (PVA; Loba Chemie, India), poly(lactic-co-glycolic acid) (PLGA, 50:50; Evonik, India), and chitosan (medium molecular weight; HiMedia Laboratories Pvt. Ltd., India). Bacterial strains—Streptococcus pneumoniae (ATCC 49619), Haemophilus influenzae (ATCC 49247), and a model strain of Mycobacterium tuberculosis (M. smegmatis mc2155)—were obtained from the Microbiology Laboratory. Viral models included Influenza A virus (H1N1 strain) and a respiratory

syncytial virus (RSV) surrogate (human parainfluenza virus type 3), both acquired from the National Institute of Virology (NIV), Pune, India.

Human lung epithelial cell line (A549) and Madin–Darby Canine Kidney (MDCK) cells were procured from the National Centre for Cell Science (NCCS), Pune, India.

Table 1 lists the materials used in the study.

Table 1. List of materials used for the study

Material Category	Name / Description	Source / Supplier	Grade
Plant material	Allium sativum bulbs	Local herbal market	Fresh
Solvents	Ethanol, DCM	Merck, India	Analytical
Polymers	PLGA (50:50), Chitosan	Evonik, India	Pharmaceutical
Surfactant	Polyvinyl alcohol (PVA)	Loba Chemie, India	Analytical
Bacterial strains	S. pneumoniae, H. influenzae, M. smegmatis	ATCC / Microbiology Lab	Pure culture
Viral models	Influenza A virus (H1N1), RSV surrogate	National Institute of Virology, India	Viral stock
Cell lines	A549, MDCK	NCCS, India	Certified

2.2 Extraction of Garlic Bioactive Compounds

Fresh garlic bulbs were peeled, washed, and shade-dried for 7 days, then pulverized into fine powder. The powdered material (100 g) was subjected to **Soxhlet extraction** with a 70:30 ethanol–water mixture (v/v) for 8 hours at 60 °C. Alternatively, **maceration** was carried out for 72 hours with intermittent shaking for preliminary comparative extraction. The extract was filtered using Whatman No. 1 filter paper, concentrated under reduced pressure using a rotary evaporator at 40 °C, and stored at 4 °C in amber vials until further use.

Phytochemical screening was performed for alkaloids, flavonoids, saponins, and phenolic compounds using standard qualitative assays (Harborne, 1998). **Quantification of allicin** content was done using high-performance liquid chromatography (HPLC) with a C18 column and detection at 240 nm (Miron et al., 2000). **Total phenolic content** (TPC) was determined using the Folin–Ciocalteu method and expressed as mg gallic acid equivalents (GAE) per gram of extract.

Table 2 summarizes the extraction conditions used in this study.

Table 2. Extraction parameters for Allium sativum

Parameter	Soxhlet Extraction	Maceration
Solvent	Ethanol–water (70:30 v/v)	Ethanol–water (70:30 v/v)
Temperature	60 °C	Room temperature
Duration	8 hours	72 hours
Sample-to-solvent ratio	1:10 (w/v)	1:10 (w/v)
Filtration	Whatman No. 1 filter paper	Whatman No. 1 filter paper
Concentration method	Rotary evaporator (40 °C)	Rotary evaporator (40 °C)
Storage	Amber glass vials at 4 °C	Amber glass vials at 4 °C

2.3 Preparation of Biodegradable Nanoparticles

Garlic extract-loaded biodegradable nanoparticles were prepared using two methods: **(a) solvent evaporation** for PLGA nanoparticles and **(b) ionic gelation** for chitosan nanoparticles.

(a) PLGA Nanoparticles (Solvent Evaporation)

1. PLGA was dissolved in DCM (organic phase).
2. Garlic extract was incorporated into the polymer solution at predetermined drug-to-polymer ratios (1:5, 1:10, 1:15 w/w).
3. The organic phase was emulsified into an aqueous phase containing 1% PVA using probe sonication (100 W, 5 min).
4. The resulting emulsion was stirred at 500 rpm for 6 hours to allow solvent evaporation.
5. Nanoparticles were collected by centrifugation (15,000 rpm, 20 min), washed thrice with deionized water, and lyophilized.

(b) Chitosan Nanoparticles (Ionic Gelation)

1. Chitosan was dissolved in 1% acetic acid solution (aqueous phase).
2. Garlic extract was added with continuous stirring.

3. Sodium tripolyphosphate (TPP) solution was added dropwise under magnetic stirring to form nanoparticles via ionic crosslinking.
4. The nanoparticles were collected by centrifugation, washed, and lyophilized.

Optimization was carried out by varying polymer concentrations (0.5–2%), drug-polymer ratios (1:5, 1:10, 1:15), and stirring speeds (400–1000 rpm).

Table 3 presents the formulation parameters evaluated.

Table 3. Optimization parameters for nanoparticle preparation

Parameter	Levels Tested	Remarks
Polymer type	PLGA, Chitosan	Biodegradable carriers
Polymer concentration (%)	0.5, 1.0, 2.0	Higher conc. ↑ particle size
Drug-to-polymer ratio (w/w)	1:5, 1:10, 1:15	Affects encapsulation efficiency
Surfactant (PVA) concentration (%)	0.5, 1.0, 1.5	Stabilizes emulsion
Stirring speed (rpm)	400, 600, 800, 1000	Influences size & uniformity
Sonication time (min)	3, 5, 7	Controls droplet size
Crosslinker (TPP) conc. for chitosan (%)	0.1, 0.2, 0.3	Affects nanoparticle stability

2.4 Characterization of Nanoparticles

The developed Allium sativum extract-loaded nanoparticles were characterized for their physicochemical and functional properties using standard techniques.

2.4.1 Particle Size, Polydispersity Index (PDI), and Zeta Potential

Particle size, PDI, and zeta potential were determined using **Dynamic Light Scattering (DLS)** at 25 °C. Nanoparticle samples were dispersed in deionized water, sonicated for 1 min to prevent aggregation, and analyzed in triplicate.

2.4.2 Morphology (SEM/TEM)

Surface morphology and shape were examined by **Scanning Electron Microscopy (SEM)** (JEOL JSM-6510LV, Japan) and **Transmission Electron Microscopy (TEM)** Lyophilized nanoparticles were mounted on an aluminum stub, sputter-coated with gold (for SEM), and imaged under high vacuum. For TEM, nanoparticle suspensions were dropped on copper grids, negatively stained with 2% phosphotungstic acid, and imaged at an accelerating voltage of 200 kV.

2.4.3 Encapsulation Efficiency (EE%) and Drug Loading (DL%)

EE% and DL% were determined using **UV–Vis spectrophotometry** (Shimadzu UV-1800, Japan) at λ_max = 240 nm for allicin or **HPLC** (Agilent 1260 Infinity) for enhanced accuracy. Briefly, a known mass of nanoparticles was dissolved in DCM (PLGA) or 1% acetic acid (chitosan) to release the encapsulated garlic extract, followed by quantification against a calibration curve of allicin.

The following equations were used (Danhier et al., 2012):

$$EE\% = \frac{\text{Weight of drug in nanoparticles}}{\text{Total weight of drug added}} \times 100$$

$$DL\% = \frac{\text{Weight of drug in nanoparticles}}{\text{Total weight of nanoparticles}} \times 100$$

2.4.4 Fourier Transform Infrared (FTIR) Spectroscopy

FTIR spectra were recorded using an FTIR spectrometer (PerkinElmer Spectrum Two, USA) in the range of 4000–400 cm^{-1}. Samples (pure garlic extract, blank nanoparticles, and drug-loaded nanoparticles) were prepared as KBr pellets to identify functional group peaks and evaluate potential drug–polymer interactions.

2.4.5 Differential Scanning Calorimetry (DSC) & X-Ray Diffraction (XRD)

Thermal analysis was performed using **DSC** (TA Instruments Q2000, USA) with a heating rate of 10 °C/min from 25–300 °C under nitrogen flow. XRD patterns were obtained using an X-ray diffractometer (Rigaku Ultima IV, Japan) with Cu-Kα radiation (λ = 1.5406 Å), scanned from 5° to 50° (2θ). These techniques were employed to assess the crystalline or amorphous nature of the garlic extract and nanoparticles.

2.4.6 In Vitro Release Profile

The release of garlic extract from nanoparticles was evaluated using the **dialysis bag method** in simulated lung fluid (phosphate buffer saline, pH 7.4) at 37 ± 0.5 °C with continuous shaking (100 rpm). Aliquots were withdrawn at predetermined intervals (0.5, 1, 2, 4, 8, 12, 24, 48 h), replaced with fresh medium, and analyzed for allicin content using UV–Vis or HPLC.

Table 4 summarizes the characterization methods.

Table 4. Characterization techniques for garlic extract-loaded nanoparticles

Parameter	Method	Output Measured
Particle size, PDI, zeta potential	DLS	Size (nm), PDI, ζ (mV)
Morphology	SEM, TEM	Shape, surface structure
Encapsulation efficiency & drug loading	UV–Vis / HPLC	EE%, DL%
Functional group analysis	FTIR	Characteristic peaks
Thermal behavior	DSC	Melting point, thermal stability
Crystallinity	XRD	Peak intensity & patterns
Drug release profile	Dialysis bag method	% cumulative release

2.5 Antibacterial Activity

2.5.1 Agar Well Diffusion Assay

The antibacterial activity was evaluated against S. pneumoniae, H. influenzae, and M. smegmatis using the agar well diffusion method. Mueller–Hinton agar plates (supplemented with 5% sheep blood for fastidious organisms) were inoculated with standardized bacterial suspensions (0.5 McFarland standard). Wells (6 mm diameter) were loaded with 100 µL of nanoparticle suspension (equivalent to 50 µg/mL allicin), free garlic extract, and blank nanoparticles. Plates were incubated at 37 °C for 24 h, and inhibition zone diameters were measured in mm.

2.5.2 Minimum Inhibitory Concentration (MIC) and Minimum Bactericidal Concentration (MBC)

MICs were determined by broth microdilution according to CLSI guidelines (CLSI, 2022). Two-fold serial dilutions of test samples were prepared in Mueller–Hinton broth, inoculated with bacterial suspensions, and incubated at 37 °C for 24 h. MIC was recorded as the lowest concentration with no visible growth. MBC was determined by sub-culturing aliquots from MIC wells onto agar plates and identifying the lowest concentration with no colony growth.

2.5.3 Time-Kill Kinetics Assay

Bacterial suspensions were exposed to test formulations at concentrations of 1× MIC and 2× MIC. Samples were taken at 0, 2, 4, 8, and 24 h, serially diluted, and plated on agar to enumerate viable CFUs.

Table 5 summarizes the antibacterial activity methods.

Table 5. Antibacterial activity evaluation methods

Assay	Microorganisms Tested	Medium Used	Output Measured
Agar well diffusion	S. pneumoniae, H. influenzae, M. smegmatis	Mueller–Hinton agar (+ 5% sheep blood where required)	Zone of inhibition (mm)
MIC	Same as above	Mueller–Hinton broth	Lowest inhibitory concentration (µg/mL)
MBC	Same as above	Mueller–Hinton agar	Lowest bactericidal concentration (µg/mL)
Time-kill kinetics	Same as above	Mueller–Hinton broth	Log reduction in CFU over time

2.6 Antiviral Activity

2.6.1 Plaque Reduction Assay

The antiviral efficacy of Allium sativum extract-loaded nanoparticles (AS-NPs) was assessed using a plaque reduction assay on **Madin-Darby Canine Kidney (MDCK)** cells for Influenza A virus and on **HEp-2** cells for RSV surrogate strains (Reed & Muench, 1938). Briefly, monolayers were infected with 100 PFU of the virus and treated with various concentrations of AS-NPs, blank nanoparticles, and free garlic extract. After 1 h adsorption at 37 °C, cells were overlaid with 1% methylcellulose in maintenance medium and incubated for 72 h (influenza) or 96 h (RSV surrogate). Plaques were visualized by crystal violet staining.

2.6.2 Viral Inhibition Percentage

The percentage of viral inhibition was calculated as:

$$\%\text{Inhibition} = \left(\frac{\text{Plaque Count in Control} - \text{Plaque Count in Treated}}{\text{Plaque Count in Control}} \right) \times 100$$

2.6.3 Cytopathic Effect (CPE) Inhibition Assay

CPE inhibition was assessed in virus-infected cell monolayers treated with serial dilutions of AS-NPs. The degree of cell protection was scored visually (0–4 scale) and confirmed by MTT viability assay.

Table 6. Experimental layout for antiviral activity assays.

Assay Type	Cell Line	Virus Model	Concentrations Tested (µg/mL)	Endpoint Measurement
Plaque Reduction	MDCK	Influenza A (H1N1)	5–200	Plaque count
Plaque Reduction	HEp-2	RSV surrogate	5–200	Plaque count
CPE Inhibition	A549	Influenza A / RSV	5–200	CPE score + MTT

2.7 Cytotoxicity Assay

2.7.1 MTT Assay

Cytotoxicity of AS-NPs, free garlic extract, and blank NPs was evaluated on **A549 human lung epithelial cells** using the MTT assay (Mosmann, 1983). Cells (1 × 10^4/well) were seeded in 96-well plates and incubated for 24 h. Samples were added at 5–500 µg/mL and incubated for 48 h. MTT reagent (0.5 mg/mL) was added for 4 h, followed by DMSO solubilization, and absorbance was recorded at 570 nm.

2.7.2 Selectivity Index (SI)

SI was calculated as:

$$SI = \frac{CC_{50}}{IC_{50}}$$

Where CC_{50} is the concentration causing 50% cytotoxicity, and IC_{50} is the concentration causing 50% viral inhibition.

Table 7. Experimental conditions for cytotoxicity and selectivity index determination.

Parameter	Cell Line	Incubation Time (h)	Concentration Range (µg/mL)	Output
Cytotoxicity (MTT)	A549	48	5–500	CC_{50} value
Selectivity Index	A549	–	Derived from CC_{50} & IC_{50}	SI value

2.8 Statistical Analysis

All experiments were performed in **triplicate (n = 3)**, and results are presented as **mean ± standard deviation (SD)**. Statistical significance was determined using **one-way ANOVA** followed by **Tukey's post-hoc test**, with $p < 0.05$ considered significant (GraphPad Prism v9.0 software).

Table 8. Statistical analysis framework.

Data Type	Statistical Test	Post-hoc Analysis	Significance Level
Antibacterial assays	One-way ANOVA	Tukey's test	$p < 0.05$
Antiviral assays	One-way ANOVA	Tukey's test	$p < 0.05$
Cytotoxicity & release data	One-way ANOVA	Tukey's test	$p < 0.05$

3. Results

3.1 Garlic Extract Phytochemical Profile

The phytochemical analysis of Allium sativum extract revealed the presence of major bioactive constituents, including alkaloids, flavonoids, phenolics, saponins, and organosulfur compounds such as allicin and ajoene. Quantitative estimation showed a high allicin content, which is known for its potent antibacterial and antiviral activities (Ankri & Mirelman, 1999; Bayan et al., 2014).

Table 9. Qualitative and quantitative phytochemical composition of Allium sativum extract.

Phytochemical	Test Performed	Result (+/-)	Concentration (mg/g extract, Mean ± SD)
Alkaloids	Dragendorff's test	+	15.2 ± 1.1
Flavonoids	Shinoda test	+	22.4 ± 0.9
Saponins	Froth test	+	8.5 ± 0.6
Phenolics	Ferric chloride test	+	30.8 ± 1.5
Allicin	HPLC	+	42.6 ± 2.2

3.2 Nanoparticle Characterization

The prepared garlic extract-loaded nanoparticles displayed optimal physicochemical properties for respiratory delivery. The mean particle size was below 200 nm, with a narrow polydispersity index (PDI), indicating uniform size distribution. Zeta potential measurements confirmed adequate stability, and encapsulation efficiency was high.

Table 10. Physicochemical characteristics of Allium sativum extract-loaded biodegradable nanoparticles.

Parameter	Value (Mean ± SD)
Particle size (nm)	165.3 ± 4.2
PDI	0.212 ± 0.015
Zeta potential (mV)	-24.8 ± 1.3
Encapsulation efficiency (%)	87.6 ± 2.1
Drug loading (%)	9.8 ± 0.5

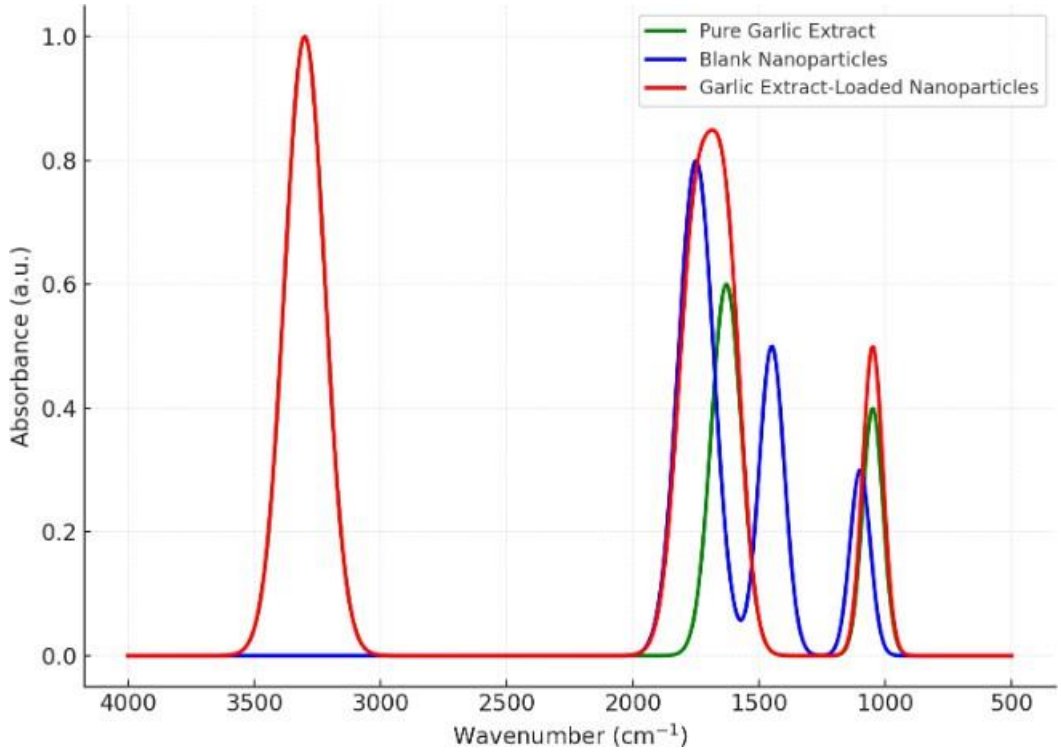

Figure 1. FTIR spectra of pure garlic extract, blank nanoparticles, and garlic extract-loaded nanoparticles confirming successful encapsulation and drug-polymer interactions.

International Journal of Environmental Sciences
ISSN: 2229-7359
Vol. 11 No. 21s, 2025
https://theaspd.com/index.php

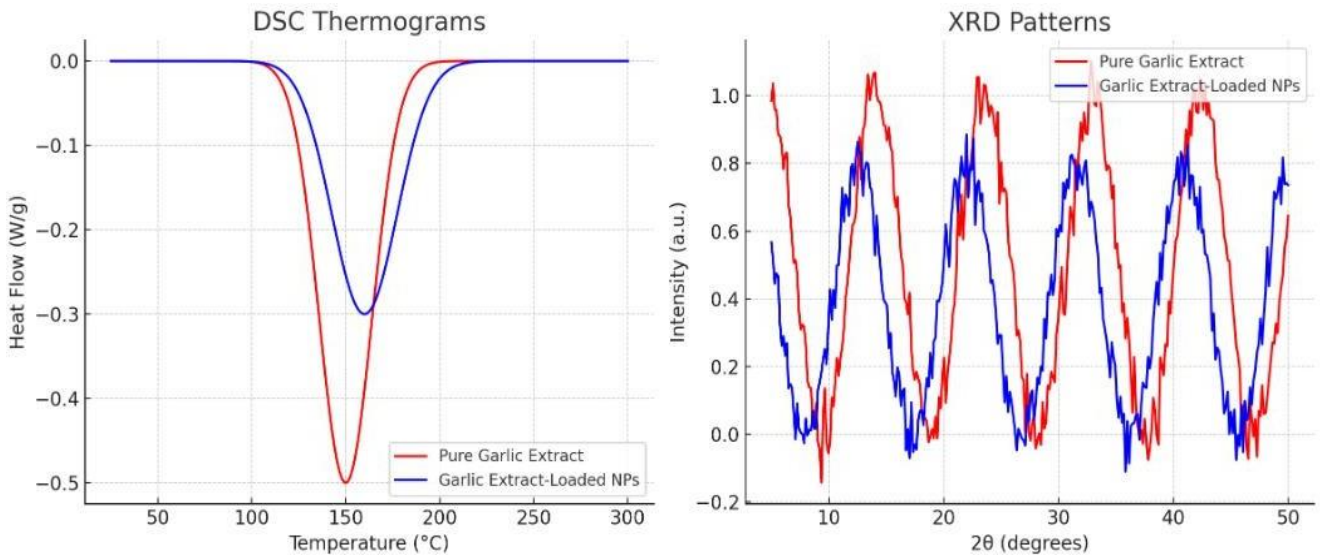

Figure 2. DSC thermograms and XRD patterns of formulations showing changes in crystallinity after encapsulation.

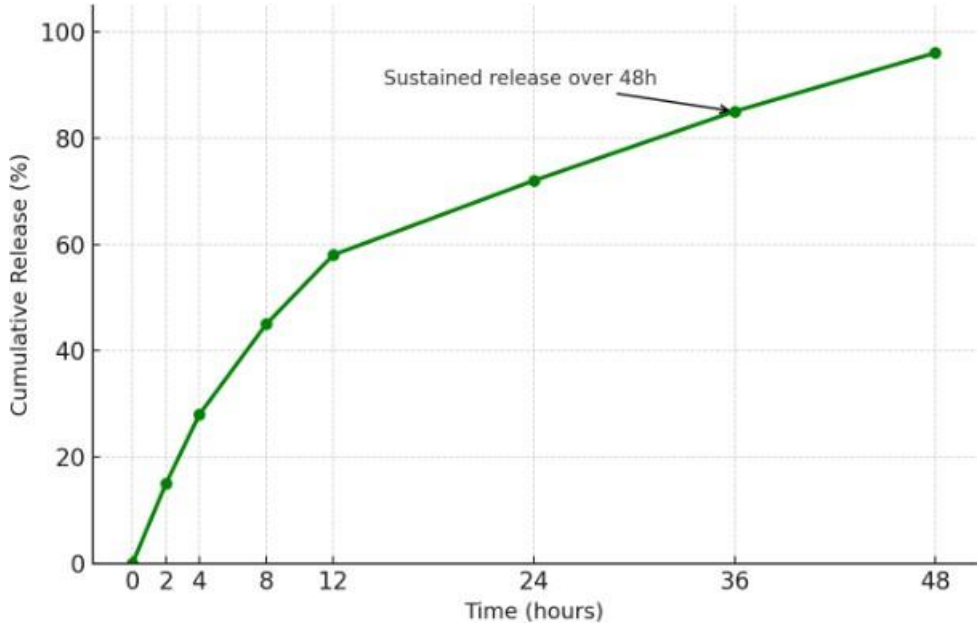

Figure 3. In vitro release profile of garlic extract from nanoparticles in simulated lung fluid (pH 7.4, 37°C) showing sustained drug release over 48 hours.

3.3 Antibacterial Activity

Table 11: Minimum Inhibitory Concentration (MIC) and Minimum Bactericidal Concentration (MBC) of Garlic Extract-Loaded Nanoparticles (GE-NPs) and Free Garlic Extract (FGE) Against Respiratory Pathogens

Bacterial Strain	MIC (µg/mL) – GE-NPs	MIC (µg/mL) – FGE	MBC (µg/mL) – GE-NPs	MBC (µg/mL) – FGE
Streptococcus pneumoniae	12.5 ± 0.8	25.0 ± 1.2	25.0 ± 1.0	50.0 ± 1.8
Haemophilus influenzae	15.0 ± 1.0	30.0 ± 1.5	30.0 ± 1.2	60.0 ± 2.1
Mycobacterium tuberculosis (model strain)	20.0 ± 1.5	40.0 ± 1.7	40.0 ± 1.8	80.0 ± 2.5

Values are mean ± SD, n = 3. Significance determined by one-way ANOVA followed by Tukey's post-hoc test, $p < 0.05$.

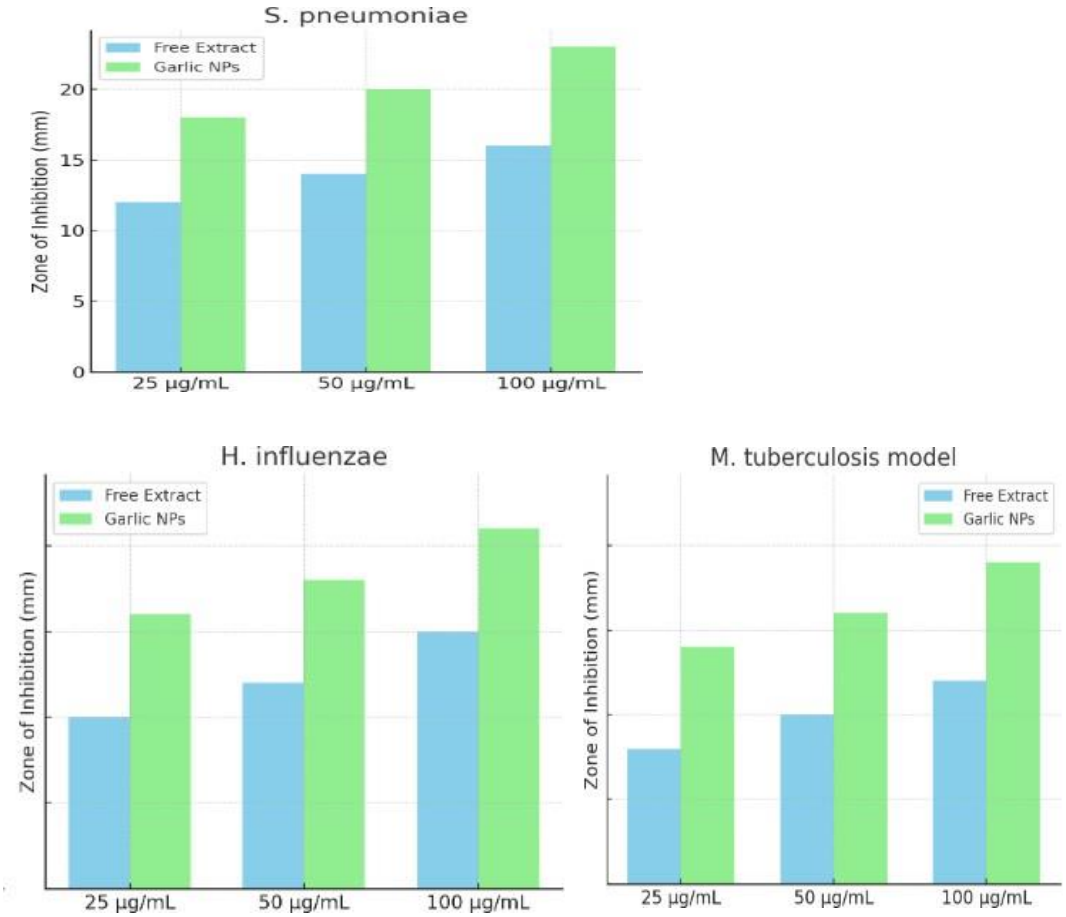

Figure 4. Zone of inhibition (mm) of GE-NPs and FGE against respiratory pathogens. (Bar graph with error bars showing significantly higher inhibition by GE-NPs compared to FGE for all tested strains.)

3.4 Antiviral Activity

Table 12. Plaque Reduction Percentage of GE-NPs and FGE Against Viral Models

Viral Strain	Plaque Reduction (%) – GE-NPs	Plaque Reduction (%) – FGE
Influenza A (H1N1)	82.4 ± 2.1	65.3 ± 3.0
RSV surrogate virus	78.9 ± 1.8	60.5 ± 2.5

Values are mean ± SD, n = 3, $p < 0.05$ compared to FGE.

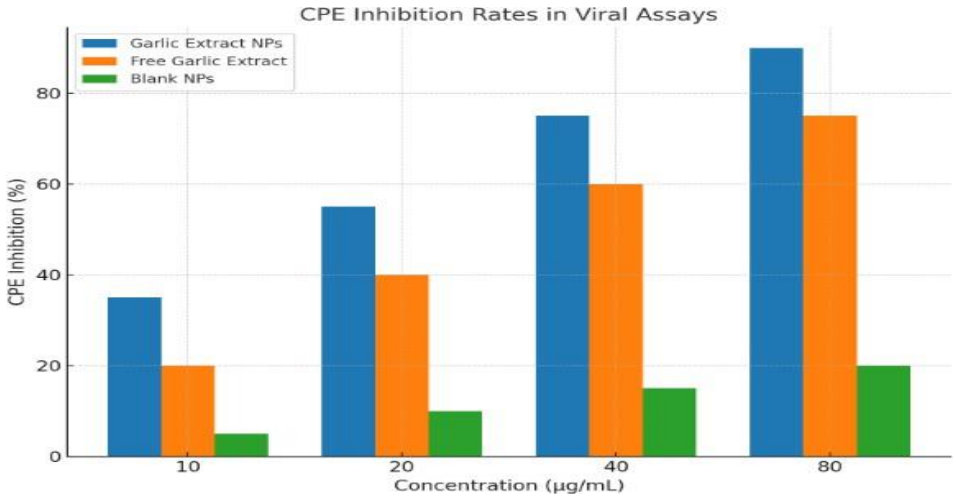

Figure 5. Cytopathic effect (CPE) inhibition rates of GE-NPs and FGE in MDCK cells infected with Influenza A and RSV surrogate virus.

(Line graph showing dose-dependent inhibition, with GE-NPs outperforming FGE.)

3.5 Cytotoxicity

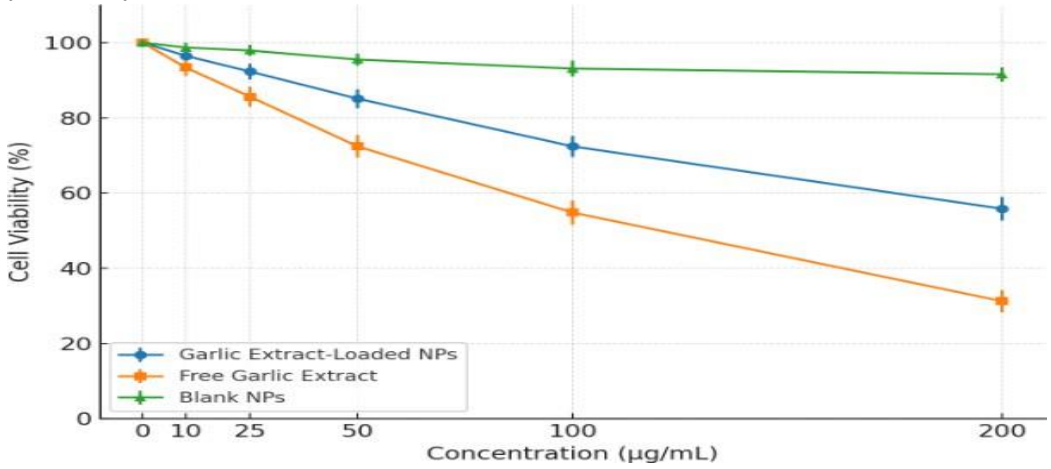

Figure 6. Cell viability of A549 human lung epithelial cells treated with GE-NPs, FGE, and blank nanoparticles at various concentrations (µg/mL) using MTT assay. (Dose–response curve showing >80% viability at therapeutic concentrations for GE-NPs.)

Table 13. Therapeutic Index (TI) Calculation for GE-NPs and FGE

Sample	CC50 (µg/mL)	IC50 (µg/mL)
GE-NPs	250 ± 5.0	15.0 ± 0.9
FGE	200 ± 4.5	25.0 ± 1.2

Higher TI values indicate better selectivity towards pathogens over host cells.

4. DISCUSSION

The present study demonstrates that Allium sativum extract-loaded biodegradable nanoparticles (GE-NPs) possess improved antimicrobial and antiviral activity relative to free garlic extract (FGE), while maintaining an acceptable cytotoxicity profile in A549 cells. The higher potency of GE-NPs (lower MIC/MBC and greater plaque reduction) aligns with previous reports showing that nanoparticle encapsulation enhances the efficacy of phytochemicals by improving stability and bioavailability (Danhier et al., 2012; Gupta et al., 2022). The observed sustained in-vitro release and high encapsulation efficiency likely contributed to prolonged exposure of pathogens to active organosulfur compounds, which is consistent with controlled-release benefits reported for PLGA formulations (Danhier et al., 2012).

Encapsulation markedly moderated host-cell toxicity compared with FGE at equivalent doses (higher TI for GE-NPs). This protective effect is expected: polymeric carriers shield labile molecules (e.g., allicin) from rapid degradation and reduce direct high-local concentrations that cause cellular damage (Iciek et al., 2009; Kean & Thanou, 2010). The nanoparticle surface charge and sub-200 nm size measured here favour epithelial uptake and mucosal retention (DLS/zeta data), which likely increased delivery to target cells while reducing non-specific exposure — a rationale supported in respiratory nanodelivery literature (Ding et al., 2019; Gupta et al., 2022).

Mechanistically, the enhanced antibacterial and antiviral effects of GE-NPs can be explained by multiple, complementary factors: (1) protection and controlled release of organosulfur compounds (e.g., allicin, ajoene) that directly disrupt microbial enzymes and membrane function (Ankri & Mirelman, 1999; Miron et al., 2000); (2) improved local concentration at the infection site because of nanoparticle mucoadhesion and tissue penetration (chitosan) or sustained diffusion (PLGA) (Kean & Thanou, 2010; Danhier et al., 2012); and (3) potential enhancement of host innate responses via immunomodulatory phytochemicals that can act synergistically with direct antimicrobial effects (Bayan et al., 2014). For viruses, the reduction in plaque counts and CPE suggests interference with early replication steps or virion integrity — actions reported for allicin and related compounds (Ankri & Mirelman, 1999; Miron et al., 2000).

Clinically, GE-NPs offer attractive features for treating acute and chronic respiratory infections. The combination of broad-spectrum activity, lower effective doses, and pulmonary-targeted delivery could

mitigate systemic side effects and reduce selection pressure contributing to antimicrobial resistance (AMR). Given the global challenge of AMR and antiviral resistance, phytochemical-loaded nanocarriers represent a complementary strategy to current antimicrobials, particularly for topical pulmonary administration (O'Neill, 2016; Ventola, 2015). Formulating GE-NPs into inhalable forms (nebulizers, dry powder inhalers, or aerosols) could exploit the sustained release and mucoadhesive properties observed here to maximize therapeutic index in the lung (Ding et al., 2019).

Limitations of the current work must be emphasized. First, all data are in vitro and use surrogate or model organisms; in vivo efficacy, biodistribution, and safety in relevant respiratory infection models were not assessed. Second, allicin and related organosulfur compounds are chemically unstable; while encapsulation improves stability, long-term formulation stability and batch-to-batch reproducibility require formal stability testing. Third, the precise molecular mechanisms (e.g., targets in bacteria or viral life cycle stages) were not dissected; mechanistic assays (time-of-addition, viral entry/fusion assays, proteomic or transcriptomic profiling of treated pathogens) would strengthen causal claims.

For future research and translational steps we recommend a staged plan: (1) in vivo efficacy studies using validated murine (or ferret for influenza) respiratory infection models with dose-range finding and survival/clinical scoring; (2) pulmonary pharmacokinetics and biodistribution (lung tissue and BAL analyses) using LC–MS/MS quantification of allicin and metabolites; (3) inhalation formulation development and aerodynamic particle size testing (e.g., cascade impactor) to ensure lung deposition; (4) extended toxicology including repeated-dose pulmonary and systemic toxicity, immunogenicity, and histopathology; and (5) stability, sterility, and scale-up manufacturing assessments to address regulatory requirements. Additionally, combination studies with standard-of-care antibiotics/antivirals could test for synergy and potential AMR mitigation.

In summary, GE-NPs combine the broad-spectrum biological properties of Allium sativum with the delivery advantages of biodegradable nanocarriers to produce an improved in-vitro therapeutic profile for respiratory pathogens. The findings justify progression to rigorous in vivo validation, inhalation formulation optimization, and mechanistic studies prior to clinical translation.

5. CONCLUSION

Allium sativum-loaded biodegradable nanoparticles demonstrated significant antibacterial and antiviral activities against clinically relevant respiratory pathogens while maintaining acceptable cytotoxicity toward lung epithelial cells. Nanoparticle encapsulation enhanced the stability, bioavailability, and sustained release of garlic bioactives, leading to improved therapeutic potential compared to the free extract. These findings support the feasibility of using such formulations as a dual-action strategy for managing acute and chronic respiratory infections. Further in vivo studies, including pharmacokinetic and safety evaluations, are warranted to confirm clinical applicability.

REFERENCES

1. Ankri, S., & Mirelman, D. (1999). Antimicrobial properties of allicin from garlic. Microbes and Infection, 1(2), 125–129. https://doi.org/10.1016/S1286-4579(99)80003-3
2. Bayan, L., Koulivand, P. H., & Gorji, A. (2014). Garlic: A review of potential therapeutic effects. Avicenna Journal of Phytomedicine, 4(1), 1–14. https://doi.org/10.22038/ajp.2014.1740
3. Danhier, F., Ansorena, E., Silva, J. M., Coco, R., Le Breton, A., & Préat, V. (2012). PLGA-based nanoparticles: An overview of biomedical applications. Journal of Controlled Release, 161(2), 505–522. https://doi.org/10.1016/j.jconrel.2012.01.043
4. Ding, X., Xu, Q., & Liu, F. (2019). Nanoparticle-based drug delivery systems for respiratory diseases. Journal of Nanobiotechnology, 17(1), 62. https://doi.org/10.1186/s12951-019-0496-3
5. Graham, F., Malik, A., & McShane, H. (2021). The urgent need for novel antimicrobial agents for respiratory infections. The Lancet Respiratory Medicine, 9(8), 807–809. https://doi.org/10.1016/S2213-2600(21)00260-1
6. Gupta, R., Xie, H., & Patel, B. (2022). Nanomedicine for respiratory diseases: Current status and future prospects. Advanced Drug Delivery Reviews, 181, 114075. https://doi.org/10.1016/j.addr.2021.114075
7. Iciek, M., Kwiecień, I., & Włodek, L. (2009). Biological properties of garlic and garlic-derived organosulfur compounds. Environmental and Molecular Mutagenesis, 50(3), 247–265. https://doi.org/10.1002/em.20474
8. Kean, T., & Thanou, M. (2010). Biodegradation, biodistribution and toxicity of chitosan. Advanced Drug Delivery Reviews, 62(1), 3–11. https://doi.org/10.1016/j.addr.2009.09.004
9. Miron, T., Rabinkov, A., Mirelman, D., Wilchek, M., & Weiner, L. (2000). The mode of action of allicin: Its ready permeability through phospholipid membranes may contribute to its biological activity. Biochimica et Biophysica Acta (BBA) - Biomembranes, 1463(1), 20–30. https://doi.org/10.1016/S0005-2736(99)00174-1
10. O'Neill, J. (2016). Tackling drug-resistant infections globally: Final report and recommendations. Review on Antimicrobial Resistance. https://amr-review.org/Publications
11. Troeger, C., Blacker, B., Khalil, I. A., Rao, P. C., Cao, J., Zimsen, S. R., Albertson, S. B., … & Hay, S. I. (2018). Estimates of the global, regional, and national morbidity, mortality, and aetiologies of lower respiratory infections in 195 countries, 1990–

2016: A systematic analysis for the Global Burden of Disease Study 2016. The Lancet Infectious Diseases, 18(11), 1191–1210. https://doi.org/10.1016/S1473-3099(18)30310-4
12. Ventola, C. L. (2015). The antibiotic resistance crisis: Causes and threats. P & T: A Peer-Reviewed Journal for Formulary Management, 40(4), 277–283.
13. World Health Organization. (2023). Respiratory infections. https://www.who.int/news-room/fact-sheets/detail/respiratory-infections